# Crystal Nucleation Using Surface-Energy-Modified Glass Substrates

Kyle A. Nordquist, Kevin M. Schaab, Jierui Sha, and Andrew H. Bond*[ORCID]

DeNovX, 3440 South Dearborn Street, Lab 204 S, Chicago, Illinois 60616, United States

**S** *Supporting Information*

**ABSTRACT:** Systematic surface energy modifications to glass substrates can induce nucleation and improve crystallization outcomes for small molecule active pharmaceutical ingredients (APIs) and proteins. A comparatively broad probe for function is presented in which various APIs, proteins, organic solvents, aqueous media, surface energy motifs, crystallization methods, form factors, and flat and convex surface energy modifications were examined. Replicate studies ($n \geq 6$) have demonstrated an average reduction in crystallization onset times of 52(4)% (alternatively 52 ± 4%) for acetylsalicylic acid from 91% isopropyl alcohol using two very different techniques: bulk cooling to 0 °C using flat surface energy modifications or microdomain cooling to 4 °C from the interior of a glass capillary having convex surface energy modifications that were immersed in the solution. For thaumatin and bovine pancreatic trypsin, a 32(2)% reduction in crystallization onset times was demonstrated in vapor diffusion experiments ($n \geq 15$). Nucleation site arrays have been engineered onto form factors frequently used in crystallization screening, including microscope slides, vials, and 96- and 384-well high-throughput screening plates. Nucleation using surface energy modifications on the vessels that contain the solutes to be crystallized adds a layer of useful variables to crystallization studies without requiring significant changes to workflows or instrumentation.
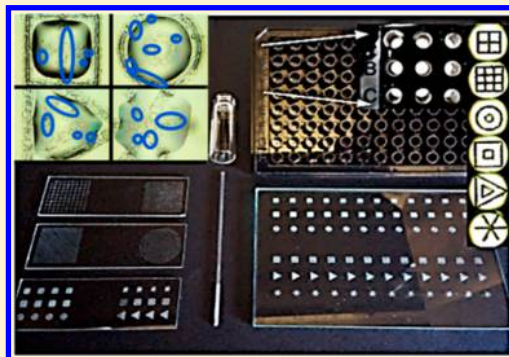
The isolation of crystalline materials continues to be a foundational aspect of chemical characterization, purification, and manufacturing.[1,2] In the field of pharmaceutical development, the cost-effective purification and predictable performance of a crystalline solid are much sought after for small molecule active pharmaceutical ingredients (APIs),[2−4] and X-ray crystal structures of biological macromolecules are fundamental to both the structure−function understanding and structure-based drug design.[5,6] Despite over a century of detailed investigation, the crystallization of new chemical entities is still largely an empirical process that often requires tens to thousands of screening experiments. The advent of 96- and 384-well plates and automated high-throughput screening (HTS) instrumentation have enabled probabilistic approaches to crystallization that involve screening large numbers of conditions to produce crystalline "hits".[7] By example, various structural biology groups have developed sophisticated automated HTS crystallization workflows over the last 15 years in order to alleviate the "crystallization bottleneck" in protein structure determination by crystallographic methods.[8,9] Despite careful optimization, the greatest attrition still occurs at the crystallization step, in which the average success rate for isolation of diffraction quality crystals hovers in the 5−7% range.[10] Only for a few sophisticated laboratories do success rates reach 15−20%,[8,11] and these confoundingly low crystallization success rates underscore the need for rational methods to improve crystallization outcomes for proteins. Advances can be expected to have a significant impact in structural biology, as >80% of the costs associated with

structure determination are incurred after the proteins have been purified.[12]

The identification of solid form variants including polymorphs, solvates, and hydrates continues to be an important and regulated aspect of small molecule API development because these different solids can have very different dissolution characteristics that can affect *in vivo* drug performance.[1−4,13,14] The needs for such crystal form screening are broad-based and will persist given that ≈90% of APIs are crystalline materials[13,15] and that ≈50−80% of small molecule APIs exhibit polymorphism at some point from discovery through manufacturing.[16−18] The many unpredictable aspects of polymorphism, and of solid form variation in general, underpin the need for rational approaches to improving crystallization outcomes for small molecule APIs, and advances here can be anticipated to help minimize the costly economic penalties incurred from untimely polymorphic transformations (e.g., Norvir, Avalide, etc.). As importantly, enhanced crystal nucleation can create value in the form of new intellectual property for commercially relevant API compositions and by making solid form screening more complete and time efficient. For example, eliminating just one month from development of a $5B blockbuster drug to yield an additional month of sales under patent can be worth more than $400M.

**Table 1. Average Crystallization Onset Times (min) for 150 mg/mL Acetylsalicylic Acid (ASA) in 91% Isopropyl Alcohol at 0 °C for Solvent and Surface Control Systems and for 20 mm Engineered Nucleation Features on Flat Glass Surfaces Immersed in Solution**

| *n* = 6 | Solvent Control | Control | Surface G18 | Surface G6 | Surface G5 | Surface CC5 |
|---|---|---|---|---|---|---|
| Avg[a] | No cryst. to 242 | 118 | 40 | 65 | 45 | 60 |
| esd[b] | No cryst. to 242 | 91 | 11 | 33 | 27 | 34 |
| Time change | --- | --- | 66% | 45% | 62% | 49% |
| Avg G18, G6, G5, CC5 | | 52 | | | | |
| esd G18, G6, G5, CC5 | | 10 | | | | |

[a]Avg = average. [b]esd = estimated standard deviation.

**Table 2. Average Crystallization Onset Times (h) for Thaumatin on 20 mm Engineered Nucleation Features at 22 °C[a]**

| *n* = 15 | Surface Control | G18 | G6 | G5 | CC5 |
|---|---|---|---|---|---|
| Avg | 44 | 32 | 33 | 37 | 39 |
| esd | 12 | 15 | 16 | 14 | 14 |
| Time change | --- | 27% | 25% | 16% | 11% |
| Avg G18, G6, G5 | | 34 | | | |
| esd G18, G6, G5 | | 2 | | | |

[a]Protein solution: 20 mg/mL thaumatin in 25 mM HEPES at pH 7.0. Precipitant solution: 0.5 M K/Na tartrate, 0.1 M sodium citrate at pH 6.3. A 10 μL total drop size with 1:1 ratio of protein:precipitant was used in sitting drop vapor diffusion.

Crystallization is often divided into the two sequential processes of nucleation and crystal growth,[1,2] with nucleation representing the best opportunity to rationally influence crystallization success rates because the thermodynamic drivers have not yet been fixed by the emergence of a crystal lattice. As the solutes in a supersaturated solution undergo the molecular recognition, aggregation, and preorganization processes that shuttle impurities, solvent, etc., out of the prenuclear aggregate, this species becomes a heterophase and presents a new surface to the supersaturated solution that interfaces with other aggregates, solvent, adventitious solids, and with the vessel or surface that contains the supersaturated solution. Vessels and other surfaces in contact with supersaturated solutions are well-known to lower the energy required to achieve heterogeneous primary nucleation,[1,11,19−21] and thus, the fluxional and growing solute aggregates can be predisposed to nucleation using appropriate solid substrates. A variety of surface coating strategies using organosilanes or self-assembled monolayers[22] has been used in crystallization; for example, the bifunctional self-assembled monolayers use directed chemical interactions with the solutes to be crystallized to give small particle sizes, narrow size distributions,[23−25] and even polymorph control.[26−28] An interesting complementary strategy that is independent of directed chemical interactions is to systematically alter the substrate surface (e.g., by etching, ablation, additive manufacturing, etc.) to give a continuum of surface energy characteristics that can facilitate nucleation through interactions between the vessel surface, the supersaturated solution, and the fluxional prenuclear aggregates therein. Such physical alterations are well-known to affect various surface properties including wettability and, by extension, the surface energy.[29−32] Considering that a supersaturated solution relieves the metastable condition by forming a suitably sized aggregate to achieve primary nucleation and recognizing that surface

energies are important in aggregate formation and growth, the convenient and systematic manipulation of surface energies in heterogeneous primary nucleation is potentially of significant utility in improving crystallization outcomes.

The promise of this platform approach derives from the ubiquity of a vessel (or substrate surface) to contain the liquid sample of the solute to be crystallized; the recognition that this surface may interact with the prenuclear solute aggregates in solution; and that the surface energy modifications can be conveniently varied and systematically produced with auto-mated manufacturing methods to give a broad spectrum of surface energies useful in crystal nucleation. By using engineered surface energy modifications to induce nucleation without the need to alter the screening chemistry, experimental workflow, or HTS equipment, this slot-in approach to enhancing nucleation promises to add a meaningful layer of variables that improve crystallization outcomes for drug development, structure-based drug design, and manufacturing. This communication presents the initial probe for function using surface energy modifications to induce nucleation and reports reproducible improvements in crystallization outcomes based on replicate investigations of various APIs, proteins, organic solvents, aqueous media, surface energy motifs, crystallization methods, form factors, and flat and convex surface energy modifications.

Table 1 shows microscopy images from the initial proof of concept studies with acetylsalicylic acid (ASA; frequently used to study new crystallization techniques[25]), in which the crystals (shown as white specks) form preferentially in the surface-energy-modified features as compared to the random distribution on the unmodified control surfaces. For the crystallization onset time studies of Table 1, solvent controls were used to rule out effects from adventitious impurities or solids (e.g., microcrystalline ASA, vessel surfaces, etc.) and

**Table 3. Average Crystallization Onset Times (h) for Bovine Pancreatic Trypsin (BPT) on 20 mm Engineered Nucleation Features at 22 °C[a]**

| n = 17 | Surface Control | G18 | G6 | G5 | CC5 |
|---|---|---|---|---|---|
| Avg | 41 | 30 | 27 | 34 | 41 |
| esd | 14 | 12 | 12 | 16 | 13 |
| Time change | --- | 27% | 34% | 17% | 0% |
| | | | | | |
| Avg G18, G6, G5 | 30 | | | | |
| esd G18, G6, G5 | 3 | | | | |

[a]Protein solution: 20 mg/mL BPT in 25 mM HEPES at pH 7.0, 10 mM CaCl$_2$, and 10 mg/mL benzamidine-HCl. Precipitant solution: 0.1 M (NH$_4$)$_2$SO$_4$, 20% (w/v) PEG 8000. A 10 $\mu$L total drop size with 1:1 ratio of protein:precipitant was used in sitting drop vapor diffusion.
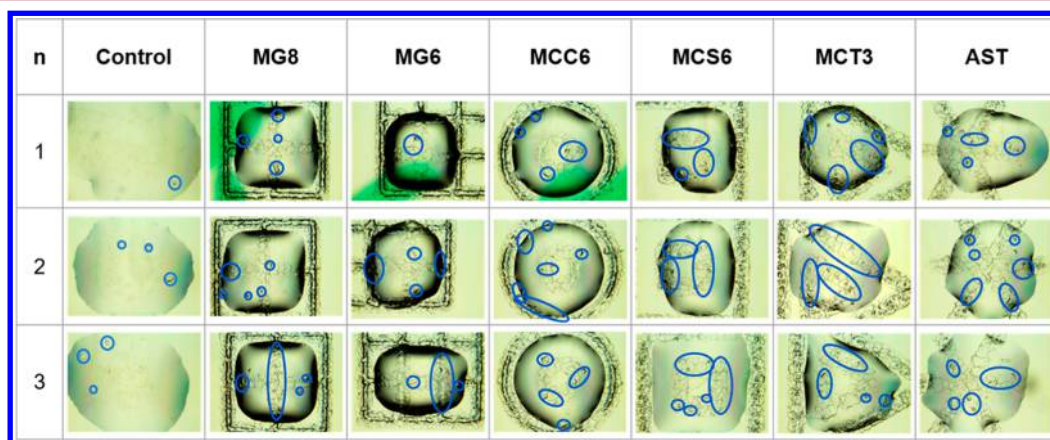


**Figure 1.** Sitting drop vapor diffusion crystallization of bovine pancreatic trypsin (BPT) on 2.5 mm surface energy modifications after 40 h at 22 °C. Protein drop: 20 mg/mL BPT in 25 mM HEPES at pH 7.0, 10 mM CaCl$_2$, 10 mg/mL benzamidine-HCl. Precipitant drop: 0.1 M (NH$_4$)$_2$SO$_4$, 20% (w/v) PEG 8000. Total drop size of 2 $\mu$L with 1:1 ratio of protein/precipitant.

surface controls (i.e., unmodified soda-lime glass microscope slides) were used to isolate effects from either the surface of the slides or the factory cut edges. For these proof of concept studies, a microscope slide serving as a control surface or one with a 20 mm surface-energy-modified nucleation site array was immersed in ≈40 mL of 150 mg/mL ASA in 91% isopropyl alcohol, the 120 mL vial sealed, and immediately quenched to 0 °C in an ice/H$_2$O bath inside a refrigerator maintained at 3 °C. As reported in Table 1, the solvent controls showed no evidence of ASA crystallization to at least 242 min, whereas the surface controls showed crystallization at 118(91) min (alternatively 118 ± 91 min) on average. Analysis of the crystallization onset time data for grids with 1.8, 0.6, and 0.5 mm square islands (i.e., G18, G6, and G5, respectively, in Table 1) and concentric circles (i.e., CC5; decrement of ≈0.5 mm between circles) shows an average 56% reduction in crystallization onset times (n = 6) and supports an expanded probe of this approach to nucleation.

Table 2 shows average crystallization onset times for the protein thaumatin (n = 15) on 20 mm grid and circular surface energy modifications using sitting drop vapor diffusion (see Supporting Information for details). The unmodified control surface produced thaumatin crystals on average at 44(12) h, with the CC5 motif of concentric circles producing little apparent reduction in crystallization time with a similar value of 39(14) h. The grid-based surface energy modifications gave progressively faster crystallization onset times of 37(14), 33(16), and 32(15) h for G5, G6, and G18, respectively, affording a reproducible maximum reduction of 27% in crystallization onset times for the G18 surface.

Tables 1 and 2 provide an initial glimpse into how the different surface energy modifications may impact crystallization of different solutes; for example, the grid motif G18 shows the largest decreases in crystallization onset times of 66% for the small molecule ASA and 27% for the protein thaumatin, whereas CC5 gives a 49% decrease for ASA and just an 11% decrease in crystallization onset time for thaumatin. While the latter is not compelling, the onset time for CC5 compares favorably to that of the surface control and is a reflection of care in the experimental approach. These data suggest that different surface energy modifications may exhibit different nucleation behavior for different solutes, and this is an important area of investigation in our laboratories.

Similarly, by analyzing the crystallization onset times for the protein bovine pancreatic trypsin (BPT; n = 17) in Table 3, it can be seen that the surface controls produced crystals at 41(14) h and that the CC5 substrate again shows little improvement in crystallization onset time at 41(13) h vs control. The grid motifs G5, G18, and G6 show decreasing crystallization onset times of 34(16), 30(12), and 27(12) h, respectively, and the surface energy profile of G6 produces the largest overall reduction in crystallization onset times for BPT of 34%.

These promising preliminary results with 20 mm surface energy modifications and 10 $\mu$L drop sizes, which are comparatively large for structural biology studies, led to the next prototype iteration resulting in surface energy modifications of 2.5 mm to accommodate a more relevant drop size of 2 $\mu$L. Figure 1 shows crystals or groups of crystals (blue circles) of BPT on the 2.5 mm surface energy motifs, and it provides an
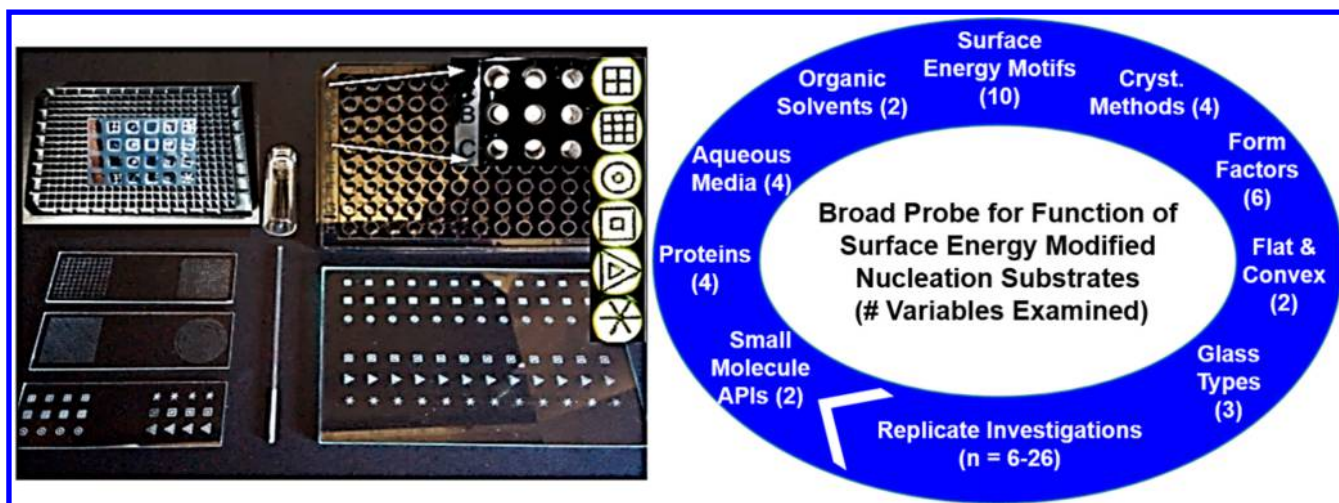
**Figure 2.** Left: Examples of surface energy modifications on various form factors including microscope slides, vials, glass capillaries, and 96- and 384-well HTS plates for crystallization. Right: Variables examined in challenging the approach.
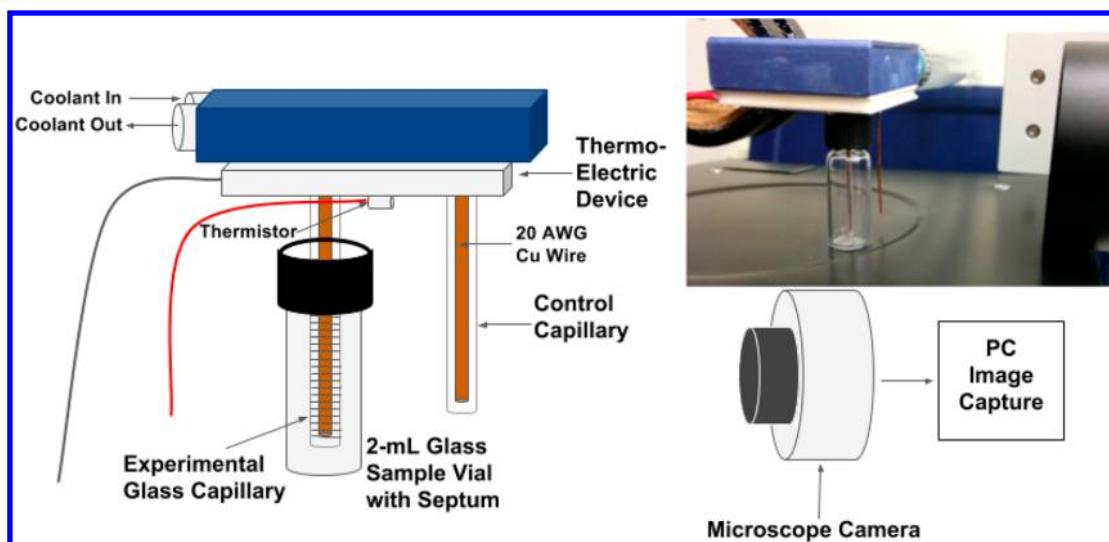


**Figure 3.** Apparatus constructed to investigate nucleation and crystallization using surface energy modifications on convex surfaces with microdomain cooling. A single 20 AWG Cu wire is fashioned into two adjacent probes and is attached to a thermoelectric device so that the thermal effect for the experimental and control surfaces is identical.

example of the naming convention: multiplexed (M), grid (G), concentric circle (CC), concentric square (CS), concentric triangle (CT), and asterisk (AST), where any trailing digit is an average (n = 3) distance between major features (peaks) in the motif. Figure 1 shows three separate crystallization trials for BPT in which one or more crystals (in blue circles) is observed on all surfaces after 40 h. More importantly, Figure 1 illustrates that the larger number of nucleation sites on the engineered surfaces results in more crystals and that these crystals are most often in contact with (i.e., adjoining or on top of) the engineered nucleation features.

The smaller footprint of the 2.5 mm nucleation site motifs allows for their convenient organization into multiplexed arrays, as shown in Figure 2 for microscope slides and various HTS plate formats for manual or automated crystallization screening. Figure 2 (right) also shows the variables examined in assessing the utility of using surface energy modification to affect crystallization outcomes. As shown, this probe for function is comparatively broad and is rigorous in using replicate studies. In a boundary probe of the experimental space, a series of

experiments was conducted that migrated away from flat form factors (Tables 1–3 and Figure 1) to the convex external surface of a glass capillary (Figure 2, bottom center). This boundary study also allowed for concurrent testing of a microdomain thermal perturbation to induce nucleation in a full immersion, batch crystallization technique. This micro-domain approach to cooling from the "interior of the solution" while the bulk is held at a separate temperature (≈22 °C in these studies) by virtue of a heat sink is one interesting approach to overcoming protein solubility issues that arise during bulk cooling protocols. Microdomain cooling effectively increases the supersaturation ratio through localized cooling, and when performed in proximity to a nucleation surface, it may promote nucleation at lower solute concentrations, which is important in structural biology where the small quantities of purified protein are often quite precious (e.g., membrane proteins). Figure 3 shows the experimental apparatus used in these preliminary studies, and results for ASA crystallization from 40% ethanol are shown in Figure 4. Here, ASA crystals are evident on the borosilicate glass capillary (left) having a linear
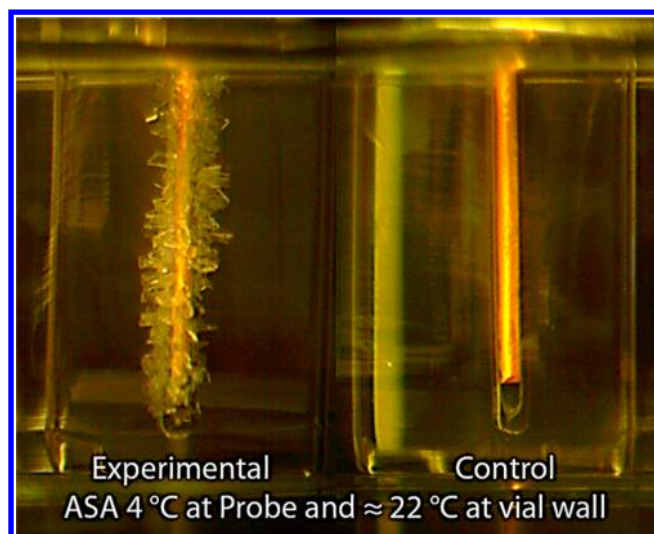
**Figure 4.** Left: Acetylsalicylic acid (ASA) crystallization from 40% ethanol on a borosilicate glass capillary with a linear array of surface-energy-modified nucleation sites. Right: Unmodified capillary as control surface. Image taken at 120 min through a $H_2O$ heat sink at 22 °C.

array of surface energy nucleation sites, as compared to the control surface (right). Table 4 shows the results of replicate quantitative studies ($n = 7$) for crystallization onset times for ASA in 91% isopropyl alcohol using the apparatus shown in Figure 3. These data show a 47% reduction in crystallization onset times from 38 to 20 min compared to control, in rigorously controlled and replicated studies. A comparison of the data in Table 4 showing an acceleration in crystallization onset times of 47% for ASA using convex surface energy modifications and a microdomain cooling approach at 4 °C with the data of Table 1 showing a 56% improvement in crystallization onset times using flat surface energy modifications and bulk cooling to 0 °C shows remarkably good agreement across these very different form factors and cooling approaches.

Figure 5 shows a time sequence in which the appearance of hen egg white lysozyme crystals became evident (white circles) with microscopic digital image capture, and these crystals largely formed and settled on the side of the capillary having the hemicircumferential surface energy modifications. The appearance of lysozyme crystals was consistently 30% faster ($n = 10$) on the surface-energy-modified capillaries cooled to 4 °C as compared to controls.[33] This microdomain cooling

technique is under continued development as a means of locally increasing supersaturation to facilitate nucleation of proteins and other molecules with challenging solubilities and/or crystallization behaviors.

The use of physical surface energy modifications to create a conveniently and systematically controlled spectrum of surface energies to facilitate nucleation in bulk solutions or in drops has been investigated in carefully controlled and replicated studies. This communication and the associated reports[33,34] discuss several tangible benefits of using surface energy modifications to induce crystal nucleation:

(1) For ASA as a model small molecule API, bulk and microdomain cooling using very different approaches and form factors (i.e., flat vs convex nucleation features) gave good agreement and an average 52(4)% reduction in crystallization onset times as compared to control surfaces.

(2) For the proteins thaumatin and BPT, maximum decreases in crystallization onset times of 27% and 34%, respectively, were observed as was an increase in the number of crystals formed per experiment, many of which formed on the surface-energy-modified nucleation arrays.

(3) Microdomain cooling in proximity to engineered surface energy modifications was shown to accelerate nucleation and appearance of crystals for ASA and lysozyme by 47% and 30%, respectively.

Systematic surface energy modifications can have beneficial effects on nucleation and crystallization outcomes, as demonstrated in this comparatively broad and rigorous probe for function that includes carefully controlled studies and $n = 6-26$ replicate crystallization trials for different small molecule APIs, proteins, organic solvents, aqueous conditions, surface energy modifications, crystallization methods, form factors, and flat and convex nucleation features. Given that nucleation relieves the metastable condition of supersaturation and that solid surfaces in contact with supersaturated solutions are known to reduce the energies needed to achieve nucleation,[1,11,19−21] the use of surface energy modifications applied to the vessel surface may be a promising new tool for use in small molecule API solid form and polymorph screening; structural biology in support of structure-based drug design; and potentially in improving the productivity and robustness of manufacturing-scale crystallization processes. Future studies with a more diverse set of APIs and proteins will allow a more quantitative assessment of the breadth and benefits of using

**Table 4. Average Crystallization Onset Times (min) for Acetylsalicylic Acid (ASA) in 91% Isopropyl Alcohol in Contact with Unmodified Capillaries as Control Surfaces and Capillaries Having a Linear Array of 19 Hemicircumferential Nucleation Motifs**[a]

| $n = 7$ | Control Surfaces | | | Experimental Surfaces | | |
|---|---|---|---|---|---|---|
| **Crystals:** | First Anywhere | On Control Capillary | On Vial Bottom | First Anywhere | On Exptl. Capillary | On Vial Bottom |
| **Avg** | 38 | 64 | 38 | 20 | 23 | 23 |
| **esd** | 31 | 59 | 31 | 20 | 19 | 23 |
| **% Change:** | | | | | | |
| **Time to First Crystals** | | | | 47% | | |
| **Time to Crystals on Capillary** | | | | 64% | | |
| **Time to Crystals on Vial Bottom** | | | | 39% | | |

[a]Each capillary was cooled to 4 °C using the device in Figure 3, while the vials were immersed in a $H_2O$ heat sink at 22 °C.
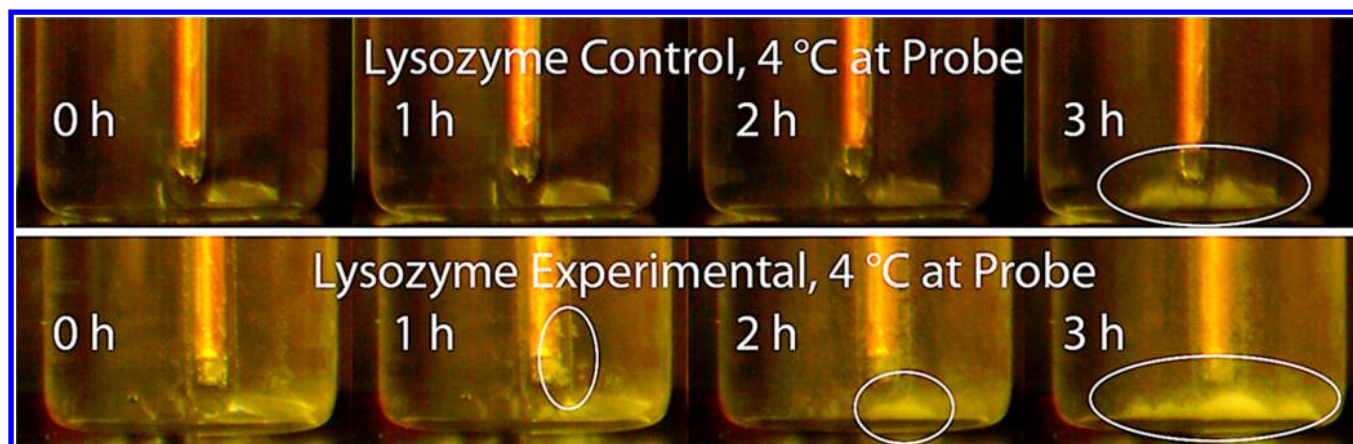
**Figure 5.** Time sequence showing crystallization of lysozyme on control surfaces (top) and capillaries with hemicircumferential surface energy modifications (bottom) using the apparatus in Figure 3.

surface energy modifications to rationally impact nucleation and improve crystallization success rates.

## ASSOCIATED CONTENT

### Ⓢ Supporting Information

The Supporting Information is available free of charge on the ACS Publications website at DOI: 10.1021/acs.cgd.7b00574.

Experimental details for crystallization protocols and microdomain cooling studies (PDF)

## AUTHOR INFORMATION

### Corresponding Author
*Phone: 910-333-6689. E-mail: abond@DeNovX.com.

### ORCID ⃝
Andrew H. Bond: 0000-0003-1526-7739

### Author Contributions
The manuscript contains contributions from all authors, all of whom have given approval to the final version of the manuscript.

### Notes
The authors declare the following competing financial interest(s): Drs. Bond and Schaab are partial owners of DeNovX and inventors on related issued and pending patents. Dr. Nordquist and Mr. Sha are employees of DeNovX.

## ABBREVIATIONS

API, active pharmaceutical ingredient; ASA, acetylsalicylic acid; Avg, average; BPT, bovine pancreatic trypsin; esd, estimated standard deviation; HTS, high throughput screening

## REFERENCES

(1) Myerson, A. S. *Handbook of Industrial Crystallization*, second ed.; Butterworth Heineman: Boston, MA, 2002.
(2) Stahl, P. H.; Wermuth, C. G. *Handbook of Pharmaceutical Salts: Properties, Selection, and Use*; Wiley-VCH: New York, 2002.
(3) *Polymorphism: In the Pharmaceutical Industry*; Hilfiker, R., Ed.; John Wiley & Sons: New York, 2006.
(4) Aaltonen, J.; Alleso, M.; Mirza, S.; Koradia, V.; Gordon, K. C.; Rantanen, J. *Eur. J. Pharm. Biopharm.* **2009**, *71*, 23.
(5) Kobilka, B. *Angew. Chem., Int. Ed.* **2013**, *52*, 6380.
(6) Moraes, I.; Evans, G.; Sanchez-Weatherby, J.; Newstead, S.; Stewart, P. D. S. *Biochim. Biophys. Acta, Biomembr.* **2014**, *1838*, 78.
(7) McPherson, A. *Methods* **2004**, *34*, 254.
(8) Kim, Y.; Babnigg, G.; Jedrzejczak, R.; Eschenfeldt, W. H.; Li, H.; Maltseva, N.; Hatzos-Skintges, C.; Gu, M.; Makowska-Grzyska, M.; Wu, R.; An, H. *Methods* **2011**, *55*, 12.
(9) Babnigg, G.; Joachimiak, A. *J. Struct. Funct. Genomics* **2010**, *11*, 71.
(10) Qiagen User's Meeting Presentation, "Protein Crystallization: An Introduction," 2010.
(11) Khurshid, S.; Govada, L.; El-Sharif, H. F.; Reddy, S. M.; Chayen, N. E. *Acta Crystallogr., Sect. D: Biol. Crystallogr.* **2015**, *71*, 534.
(12) Babnigg, G. Argonne National Laboratory-Advanced Protein Crystallization Facility, personal communication, 2014.
(13) Chen, J.; Sarma, B.; Evans, J. M.; Myerson, A. S. *Cryst. Growth Des.* **2011**, *11*, 887.
(14) Miller, S. P.; Raw, A. S.; Yu, L. X. In *Polymorphism: In the Pharmaceutical Industry*; Hilfiker, R., Ed.; John Wiley & Sons: New York, 2006.
(15) Wong, S. Y.; Tatusko, A. P.; Trout, B. L.; Myerson, A. S. *Cryst. Growth Des.* **2012**, *12*, 5701.
(16) Aldridge, S. *Chemistry World* **2007**, *4*, 64.
(17) Thayer, A. M. *Chem. Eng. News* **2007**, *85*, 31.
(18) Lee, A. Y.; Erdemir, D.; Myerson, A. S. *Annu. Rev. Chem. Biomol. Eng.* **2011**, *2*, 259.
(19) Vekilov, P. G. *Nanoscale* **2010**, *2*, 2346.
(20) Qian, M. *Acta Mater.* **2007**, *55*, 943.
(21) Nederlof, I.; Hosseini, R.; Georgieva, D.; Luo, J.; Li, D.; Abrahams, J. P. *Cryst. Growth Des.* **2011**, *11*, 1170.
(22) Pham, T.; Lai, D.; Ji, D.; Tuntiwechapikul, W.; Friedman, J. M.; Lee, T. R. *Colloids Surf., B* **2004**, *34*, 191.
(23) Kang, J. F.; Zaccaro, J.; Ulman, A.; Myerson, A. *Langmuir* **2000**, *16*, 3791.
(24) Lee, A. Y.; Ulman, A.; Myerson, A. S. *Langmuir* **2002**, *18*, 5886.
(25) Diao, Y.; Myerson, A. S.; Hatton, T. A.; Trout, B. L. *Langmuir* **2011**, *27*, 5324.
(26) Alvarez, A. J.; Singh, A.; Myerson, A. S. *Cryst. Growth Des.* **2009**, *9*, 4181.
(27) Yang, X.; Sarma, B.; Myerson, A. S. *Cryst. Growth Des.* **2012**, *12*, 5521.
(28) Kim, K.; Centrone, A.; Hatton, T. A.; Myerson, A. S. *CrystEngComm* **2011**, *13*, 1127.
(29) Bico, J.; Marzolin, C.; Quéré, D. *Europhys. Lett.* **1999**, *47*, 220.
(30) Xue, L.; Han, Y. *Prog. Polym. Sci.* **2011**, *36*, 269.

(31) Di Profio, G.; Fontananova, E.; Curcio, E.; Drioli, E. *Cryst. Growth Des.* **2012**, *12*, 3749.

(32) Zamuruyev, K. O.; Bardaweel, H. K.; Carron, C. J.; Kenyon, N. J.; Brand, O.; Delplanque, J. P.; Davis, C. E. *Langmuir* **2014**, *30*, 10133.

(33) Nordquist, K. A.; Schaab, K. M.; Bond, A. H. Manuscript in preparation, 2017.

(34) Bond, A. H.; Schaab, K. M. U.S. Patent 9,193,664, 2015.